Article
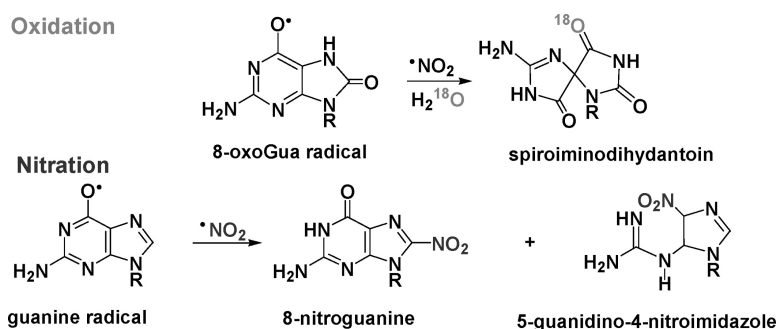
Combination of Nitrogen Dioxide Radicals with 8-Oxo-7,8-dihydroguanine and Guanine Radicals in DNA: Oxidation and Nitration End-Products

Richard Misiaszek, Conor Crean, Nicholas E. Geacintov, and Vladimir Shafirovich

More About This Article

Additional resources and features associated with this article are available within the HTML version:

- Supporting Information
- Links to the 6 articles that cite this article, as of the time of this article download
- Access to high resolution figures
- Links to articles and content related to this article
- Copyright permission to reproduce figures and/or text from this article

View the Full Text HTML

Combination of Nitrogen Dioxide Radicals with 8-Oxo-7,8-dihydroguanine and Guanine Radicals in DNA: Oxidation and Nitration End-Products

Richard Misiaszek, Conor Crean, Nicholas E. Geacintov, and Vladimir Shafirovich*

Contribution from the Chemistry Department and Radiation and Solid State Laboratory, 31 Washington Place, New York University, New York, New York 10003-5180

Received September 15, 2004; E-mail: vs5@nyu.edu

Abstract: The oxidation and nitration reactions in DNA associated with the combination of nitrogen dioxide radicals with 8-oxo-7,8-dihydroguanine (8-oxoGua) and guanine radicals were explored by kinetic laser spectroscopy and mass spectrometry methods. The oxidation/nitration processes were triggered by photoexcitation of 2-aminopurine (2AP) residues site-specifically positioned in the 2′-deoxyribooligonucleotide 5′-d(CC[2AP]TC**[X]**CTACC) sequences (X = 8-oxoGua or G), by intense 308 nm excimer laser pulses. The photoionization products, 2AP radicals, rapidly oxidize either 8-oxoGua or G residues positioned within the same oligonucleotide but separated by a TC dinucleotide step on the 3′-side of 2AP. The two-photon ionization of the 2AP residue also generates hydrated electrons that are trapped by nitrate anions thus forming nitrogen dioxide radicals. The combination of nitrogen dioxide radicals with the 8-oxoGua and G radicals occurs with similar rate constants ($\sim 4.3 \times 10^8$ M^{-1} s^{-1}) in both single- and double-stranded DNA. In the case of 8-oxoGua, the major end-products of this bimolecular radical−radical addition are spiroiminodihydantoin lesions, the products of 8-oxoGua oxidation. Oxygen-18 isotope labeling experiments reveal that the O-atom in the spiroiminodihydantoin lesion originates from water molecules, not from nitrogen dioxide radicals. In contrast, combination of nitrogen dioxide and guanine neutral radicals generated under the same conditions results in the formation of the nitro products, 5-guanidino-4-nitroimidazole and 8-nitroguanine adducts. The mechanistic aspects of the oxidation/nitration processes and their biological implications are discussed.

Introduction

The oxidative stress developed in response to environmental pollutants, chronic inflammation, and various degenerative diseases generate oxidative modifications (lesions) of DNA molecules that are believed to increase the risk of malignant cell transformation and the development of many human cancers.[1−3] The most common DNA lesion detected in vivo is 8-oxo-7,8-dihydroguanine (8-oxoGua), the product of a two-electron oxidation of guanine bases.[1,4] The 8-oxoGua lesion is more easily oxidizable than any of the natural nucleic acid bases.[5,6] Nitrogen dioxide, one of the important and ubiquitous free radicals in biological systems,[3,7] is a potential candidate for the selective oxidation of 8-oxoGua residues in vivo. The reduction potential of nitrogen dioxide,[8] $E° = 1.04$ V vs NHE, is greater than the midpoint oxidation potential of 8-oxo-7,8-

dihydro-2′-deoxyguanosine (8-oxodGuo),[9] $E_7 = 0.74$ V vs NHE, but less than that of 2′-deoxyguanosine (dG),[10] $E_7 = 1.29$ V vs NHE. The values of these redox potentials suggest that the further selective one-electron oxidation of 8-oxoGua by $•NO_2$ may be feasible even in the presence of an excess of guanine residues. Indeed, our own laser flash photolysis experiments demonstrated that $•NO_2$ radicals oxidize 8-oxodGuo and do not show any observable reactivities with any of the four normal nucleobases in DNA.[11] However, the direct one-electron oxidation of 8-oxodGuo by $•NO_2$ to generate 8-oxoGua radicals is unsuitable for studying the reaction kinetics of the latter because the reaction rate constant of 8-oxoGua with $•NO_2$ ($k \sim 5 \times 10^6$ M^{-1} s^{-1}) is much slower than the rate constants of the subsequent chemical reactions, a situation that provides little insight into reactivities of 8-oxoGua radicals themselves. Although the 8-oxodGuo$^{•+}$/8-oxodGuo(−H)$^{•}$ radicals derived from the one-electron oxidation of 8-oxodGuo by $•NO_2$ were identified by direct time-resolved spectroscopic methods,[11] neither the rates of their decay nor the nature of the end-products derived from the attack of 8-oxoGua by $•NO_2$ radicals has been characterized.

(1) Beckman, K. B.; Ames, B. N. *J. Biol. Chem.* **1997**, *272*, 19633−19636.
(2) Grisham, M. B.; Jourd'heuil, D.; Wink, D. A. *Aliment. Pharmacol. Ther.* **2000**, *14 Suppl 1*, 3−9.
(3) Dedon, P. C.; Tannenbaum, S. R. *Arch. Biochem. Biophys.* **2004**, *423*, 12−22.
(4) Beckman, K. B.; Ames, B. N. *Mutat. Res.* **1999**, *424*, 51−58.
(5) Cadet, J.; Bellon, S.; Berger, M.; Bourdat, A. G.; Douki, T.; Duarte, V.; Frelon, S.; Gasparutto, D.; Muller, E.; Ravanat, J. L.; Sauvaigo, S. *Biol. Chem.* **2002**, *383*, 933−943.
(6) Hickerson, R. P.; Prat, F.; Muller, J. G.; Foote, C. S.; Burrows, C. J. *J. Am. Chem. Soc.* **1999**, *121*, 9423−9428.
(7) Augusto, O.; Bonini, M. G.; Amanso, A. M.; Linares, E.; Santos, C. C.; De Menezes, S. L. *Free Radical Biol. Med.* **2002**, *32*, 841−859.
(8) Stanbury, D. M. *Adv. Inorg. Chem.* **1989**, *33*, 69−138.

(9) Steenken, S.; Jovanovic, S. V.; Bietti, M.; Bernhard, K. *J. Am. Chem. Soc.* **2000**, *122*, 2373−2374.
(10) Steenken, S.; Jovanovic, S. V. *J. Am. Chem. Soc.* **1997**, *119*, 617−618.
(11) Shafirovich, V.; Cadet, J.; Gasparutto, D.; Dourandin, A.; Geacintov, N. E. *Chem. Res. Toxicol.* **2001**, *14*, 233−241.
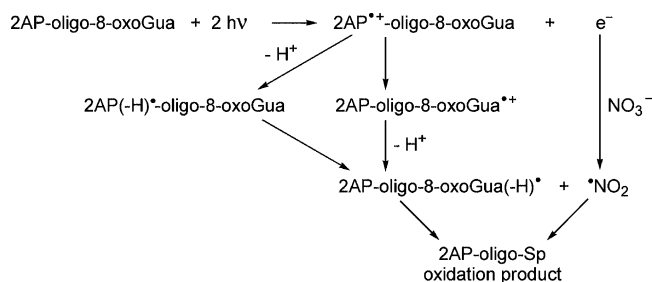
Figure 1. Schematic representation of the photochemical generation of 8-oxoGua and nitrogen dioxide radicals via the two-photon photoionization of 2-aminopurine and their subsequent combination reactions leading to end-products in aqueous DNA solutions.

In this work, 2-aminopurine (2AP), a nucleic acid base analogue, and 8-oxoGua have been incorporated into 2′-deoxyribooligonucleotide strands at defined sites separated by a TC dinucleotide step.[12] Intense 308 nm laser pulse excitation of these oligonucleotides in either the single- or double-stranded forms in aqueous solutions induces a two-photon ionization of the 2AP residues yielding $2AP^{\bullet+}$ radical cations and hydrated electrons (Figure 1). Under these conditions of photoexcitation, neither 8-oxoGua nor the four normal DNA nucleobases are photoionized.[12] The $2AP^{\bullet+}$ radicals rapidly deprotonate to yield the neutral $2AP(-H)^{\bullet}$ radicals. Both the $2AP^{\bullet+}$ and $2AP(-H)^{\bullet}$ radicals are strong one-electron oxidants that selectively oxidize 8-oxoGua at a distance.[12]

The deoxygenated solutions contained NO_3^- anions that, in the absence of O_2, rapidly and quantitatively scavenge the hydrated electrons derived from the photoionization of 2AP, thus resulting in the formation of $^{\bullet}NO_2$ radicals.[13] We utilized time-resolved spectroscopic methods to monitor the disappearance of the $^{\bullet}NO_2$ and $8\text{-oxoGua}^{\bullet+}/8\text{-oxoGua}(-H)^{\bullet}$ radicals that reacted predominantly by combining with one another. The oxidative character of these combination reactions was confirmed by isolating the end-products by reversed-phase HPLC methods and by identifying the products by MALDI-TOF/MS and HPLC-ESI/MS methods. The major product found was the spiroiminodihydantoin (Sp) lesion,[14−18] the product of a two-electron oxidation of the 8-oxoGua residues (Figure 1). In contrast, the combination reactions of $^{\bullet}NO_2$ with the guanine neutral radicals, $G(-H)^{\bullet}$, generated the nitration products, 8-nitroguanine (8-nitroGua)[19−21] and 5-guanidino-4-nitroimidazole (NIm)[22,23] adducts as reported earlier.[24,25]

Experimental Section

Materials. All chemicals (analytical grade) were purchased from Sigma-Aldrich Fine Chemicals; $H_2^{18}O$ (95% of ^{18}O) was from Icon Isotopes (Summit, NJ). The oligonucleotides were synthesized by standard automated phosphoramidite chemistry techniques. Phophoramidites and other chemicals required for oligonucleotide synthesis were obtained from Glen Research (Sterling, VA). To prevent the oxidation of 8-oxoGua residues, the tritylated oligonucleotides were deprotected overnight at 55 °C in concentrated aqueous ammonia solutions containing 0.25 M mercaptoethanol. The crude oligonucleotides were purified by reversed-phase HPLC, detritylated in 80% acetic acid according to standard protocols, and desalted using reversed-phase HPLC. The integrity of the oligonucleotides was confirmed by MALDI-TOF mass spectrometry.

Laser Flash Photolysis. The transient absorption spectra and kinetics of free radical reactions were monitored directly using a fully computerized kinetic spectrometer system (∼7 ns response time) described elsewhere.[26] Briefly, 308 nm nanosecond XeCl excimer laser pulses were used to photolyze the oligonucleotides in 0.25 mL phosphate buffer solutions (5 mM, pH 7.5) containing 1 mM NaNO$_3$ and 100 mM NaCl. Before laser excitation the sample solutions were thoroughly purged with argon to remove oxygen. The transient absorbance was probed along a 1 cm optical path by a light beam from a 75 W xenon arc lamp with its light beam oriented perpendicular to the laser beam. The signal was recorded by a Tektronix TDS 5052 oscilloscope operating in its high resolution mode that typically allows for a suitable signal/noise ratio after a single laser short.

The second-order rate constants of the oxidative reactions initiated by free radicals were typically determined by least-squares fits of the appropriate kinetic equations to the transient absorption profiles obtained in five different experiments with five different samples. The rate constant of 8-oxoGua oxidation by $^{\bullet}NO_2$ radicals was obtained by a numerical analysis of the growth of the $8\text{-oxoGua}(-H)^{\bullet}$ transient absorbance recorded at different concentrations of 8-oxoGua-containing oligonucleotides. This analysis was performed using the PRKIN computer programs developed by H. Schwartz at the Brookhaven National Laboratory.

Reversed-Phase HPLC. Separation of the stable end-products was performed on an analytical (250 × 4.6 mm i.d.) ACE C18 column (MAC-MOD Analytical, Chadd Ford, PA). An 8−20% linear gradient of acetonitrile in 50 mM triethylammonium acetate in water (pH 7) was utilized for 60 min at a flow rate of 1 mL/min (detection of products at 260 nm). The HPLC fractions were evaporated under vacuum to remove acetonitrile, and were purified by a second HPLC cycle. The purified adducts were desalted by reversed-phase HPLC using the following mobile phases: 5 mM triethylammonium acetate (10 min), deionized water (10 min), and an isocratic 50:50 acetonitrile and H$_2$O mixture (15 min). They were then subjected to MALDI-TOF/MS analysis.

MALDI-TOF/MS Assay of Oligonucleotides. The mass spectra of the oligonucleotides were acquired using a Bruker OmniFLEX instrument. The matrix was a 2:1 mixture of 2′,4′,6′-trihydroxy-acetophenone methanol solution (30 mg/mL) and ammonium citrate aqueous solution (100 mg/mL). The aliquots (1−2 μL) of the 10 pmol/μL desalted samples and the matrix solution were spotted on a MALDI target and air-dried before analysis. The mass spectrometer equipped with a 337 nm nitrogen laser was operated in the negative linear mode (accelerating voltage 19 kV, extraction voltage 92.7% of the accelerating voltage, ion focus 9 kV, and delay time 250 ns). Each spectrum was obtained with an average of 50−100 laser shots. The mass spectra were

(12) Shafirovich, V.; Cadet, J.; Gasparutto, D.; Dourandin, A.; Huang, W.; Geacintov, N. E. *J. Phys. Chem. B* **2001**, *105*, 586−592.
(13) Buxton, G. V.; Greenstock, C. L.; Helman, W. P.; Ross, A. B. *J. Phys. Chem. Ref. Data* **1988**, *17*, 513−886.
(14) Luo, W.; Muller, J. G.; Rachlin, E. M.; Burrows, C. J. *Org. Lett.* **2000**, *2*, 613−616.
(15) Leipold, M. D.; Muller, J. G.; Burrows, C. J.; David, S. S. *Biochemistry* **2000**, *39*, 14984−14992.
(16) Niles, J. C.; Wishnok, J. S.; Tannenbaum, S. R. *Org. Lett.* **2001**, *3*, 963−966.
(17) Sugden, K. D.; Campo, C. K.; Martin, B. D. *Chem. Res. Toxicol.* **2001**, *14*, 1315−1322.
(18) Joffe, A.; Geacintov, N. E.; Shafirovich, V. *Chem. Res. Toxicol.* **2003**, *16*, 1528−1538.
(19) Yermilov, V.; Rubio, J.; Becchi, M.; Friesen, M. D.; Pignatelli, B.; Ohshima, H. *Carcinogenesis* **1995**, *16*, 2045−2050.
(20) Tretyakova, N. Y.; Burney, S.; Pamir, B.; Wishnok, J. S.; Dedon, P. C.; Wogan, G. N.; Tannenbaum, S. R. *Mutat. Res.* **2000**, *447*, 287−303.
(21) Lee, J. M.; Niles, J. C.; Wishnok, J. S.; Tannenbaum, S. R. *Chem. Res. Toxicol.* **2002**, *15*, 7−14.
(22) Niles, J. C.; Wishnok, J. S.; Tannenbaum, S. R. *J. Am. Chem. Soc.* **2001**, *123*, 12147−12151.
(23) Gu, F.; Stillwell, W. G.; Wishnok, J. S.; Shallop, A. J.; Jones, R. A.; Tannenbaum, S. R. *Biochemistry* **2002**, *41*, 7508−7518.

(24) Shafirovich, V.; Mock, S.; Kolbanovskiy, A.; Geacintov, N. E. *Chem. Res. Toxicol.* **2002**, *15*, 591−597.
(25) Joffe, A.; Mock, S.; Yun, B. H.; Kolbanovskiy, A.; Geacintov, N. E.; Shafirovich, V. *Chem. Res. Toxicol.* **2003**, *16*, 966−973.
(26) Shafirovich, V.; Dourandin, A.; Huang, W.; Luneva, N. P.; Geacintov, N. E. *J. Phys. Chem. B* **1999**, *103*, 10924−10933.

internally calibrated by using synthetic oligonucleotides of known molecular weights.

Oxygen-18 Isotope Labeling. The oligonucleotide samples (10 nmol) in buffer solutions were evaporated to dryness and dissolved in 100 μL of $H_2^{18}O$. After irradiation at 9 °C, the spiroiminodihydantoin adducts were isolated and desalted by reversed-phase HPLC. Chemical hydrolysis of the spiroiminodihydantoin adducts was performed using a commercially available solution of hydrogen fluoride (~70%) in pyridine (HF/Pyr) as previously described.[27] The dry adduct (1−3 nmol) in a plastic vial was treated with 50 μL of HF/Pyr at 37 °C for 30 min. The reaction mixture was diluted with 1 mL of water and neutralized by a vigorous agitation with 80 mg of $CaCO_3$. The insoluble inorganic salts were removed by centrifugation. The sample was evaporated to dryness, and traces of pyridine were removed by a repeated lyophilization. The final aqueous solution (~20 μL) was passed through a Millipore centrifugal filter and subjected to HPLC-ESI/MS analysis. The authentic Sp nuclebase standards were obtained by the chemical hydrolysis (as described above) of the Sp nucleosides prepared by the photooxidation of 2′-deoxyguanosine in the presence of the methylene blue photosensitizer and separated by normal-phase HPLC.[27] The Sp diastereomers prepared by these methods and initially designated as 4-hydroxy-8-oxo-7,8-dihydroguanine[27,28] were thoroughly characterized by ESI-MS/MS methods. We found that the mass spectra recorded in the positive mode exhibited, besides the molecular ion signal ([M + H]$^+$) at *m/z* 184, characteristic signals at *m/z* 86, 114, 141, and 156 (for additional details see Supporting Information). These fragments are characteristic products of the fragmentation of Sp,[14,29] thus confirming our assignment. In agreement with the results of other groups,[14,16,29,30] the oxidation products prepared by the photosensitization of 2′-deoxyguanosine by methylene blue are thus the Sp diastereomers (not hydroxyderivatives of 8-oxoGua).
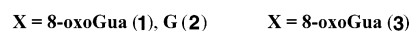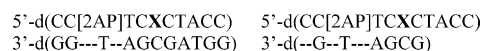
HPLC-ESI/MS Assay. These experiments were performed using an LC/MSD-trap XCT spectrometer (Agilent Technologies, Palo Alto, CA) with an Agilent 1100 Series Capillary LC System. The Sp nucleobase was separated from the nucleobase mixture on a (50 × 2 mm i.d.) Hypercarb column (Thermo-Hypersil-Keystone, Bellefonte, PA) employing the following mobile phases: water with 0.1% formic acid (5 min) and then a 0−90% linear gradient of acetonitrile in water with 0.1% formic acid for 40 min at a flow rate of 0.4 mL/min. The mass spectra were recorded in the positive mode. The nebulizer gas pressure was 40 psi, the dry gas flow rate was 8.0 L/min, and the dry temperature was set at 350 °C. The target ion abundance value was set at 50 000, and the maximum accumulation time was 50 ms. For general analytical experiments, the instrument was operated using the "smart" parameter setting and the detector was set for a particular ion of interest. Extracted ion chromatogram for *m/z* 184 and *m/z* 186 were selected to monitor unlabeled (^{16}O) and labeled (^{18}O) spiroiminodihydantoins, respectively.

Results

In this work we explore the mechanisms of oxidation of 8-oxoGua$^{•+}$/8-oxoGua(−H)$^•$ radical intermediates by combination reactions with $^•NO_2$ radicals. The kinetics of these reactions were monitored by laser kinetic spectroscopy using the characteristic absorption band of 8-oxoGua$^{•+}$/8-oxoGua(−H)$^•$ radicals at 325 nm.[9,11,12] In contrast, the molar absorptivities of $^•NO_2$ radicals are small and do not exceed 200 M^{-1} cm^{-1} in the spectral range 250−600 nm.[31] To reconfirm that these radicals

are indeed formed under our conditions, we verified that $^•NO_2$ radicals react with G(−H)$^•$ radicals to form the nitro products, 8-nitroguanine[19−21] and 5-guanidino-4-nitroimidazole adducts[22,23] detected by their characteristic absorption bands near 385 nm.[24,25] The oligonucleotide adducts derived from the reactions of $^•NO_2$ radicals were isolated by reversed-phase HPLC and identified by MALDI-TOF/MS and HPLC-ESI/MS techniques.

The DNA duplexes **1**−**3** were prepared by annealing 5′-d(CC-[2AP]TC**X**CTACC) with either of two complementary strands, 5′-d(GGTAGCGATGG) or 5′-d(GCGTAG):

5'-d(CC[2AP]TC**X**CTACC)   5'-d(CC[2AP]TC**X**CTACC)
3'-d(GG---T--AGCGATGG)   3'-d(--G--T---AGCG)

X = 8-oxoGua (1), **G (2)**   **X = 8-oxoGua (3)**

The melting temperatures of these duplexes are 44.0 ± 0.7 °C (**1**), 50.8 ± 0.7 °C (**2**), and 24.0 ± 1.0 °C (**3**) in 5 mM phosphate buffer solution (pH 7.5) containing 100 mM NaCl. The reactions of duplex **3** were studied at 9 °C to prevent the dissociation of the duplexes. At room temperature, duplex **3** partially dissociates and the two strands can be easily separated by reversed-phase HPLC methods. The full duplex **1** was utilized as a control to verify that the reaction kinetics of the radicals were not different because of the shorter complementary strand in duplex **3**. Experiments with single-stranded oligonucleotides and duplex **1** were performed at room temperature (23 ± 2) °C.

Monitoring the Oxidation/Nitration Reactions by Time-Resolved Spectroscopic Methods. Photoexcitation of the 5′-d(CC[2AP]TC**X**CTACC) sequence in either single- or double-stranded forms in deoxygenated buffer solutions (pH 7.5) with intense 308 excimer laser pulses induces a selective ionization of the 2AP residues. The laser flash photolysis experiments showed that, in agreement with previous observations, the oxidation of 8-oxoGua or G residues by 2AP radicals[12] and the scavenging of hydrated electrons by NO_3^- anions resulting in the formation of $^•NO_2$ radicals[13] is complete within ~100 μs. Therefore, the transient absorption spectra recorded on a millisecond time scale at room-temperature resemble either the spectra of the 8-oxoGua radicals (Figure 2A) that are characterized by a narrow absorption band near 325 nm[9,11,12] or the spectra of guanine radicals (Figure 2B) with an absorption maximum at 315 nm.[10,26,32−35]

The radical species observed cannot be unambiguously assigned to the radical cation or the neutral radical forms because the transient absorption spectra of these two species are very close to one another.[9,12,32] Nevertheless, based on the following assessments, the spectra recorded at pH 7.5 (Figure 2) were assigned to the neutral forms 8-oxoGua(−H)$^•$ (~90%) and G(−H)$^•$ (~100%). Indeed, the rate constant of the radical cation dissociation can be estimated as $k_- = k_+ K_a$, where k_+ is the rate constant of the radical protonation (~2×10^{10} M^{-1} s^{-1})[32] and K_a is the dissociation constant. Using the pK_a values of 6.6 for 8-oxodGuo$^{•+}$ and 3.9 for dG$^{•+}$,[9,32] the characteristic times of the radical cation deprotonation ($\tau_- = 1/k_-$) are 0.2 ms and 500 ns, respectively. Thus, deprotonation of the radical cations should be complete by the time the recording of the transient absorption spectra is started (Figure 2). Recent pulse radiolysis experiments confirmed that, even in double-stranded DNA, the

(27) Ravanat, J. L.; Cadet, J. *Chem. Res. Toxicol.* **1995**, *8*, 379−388.
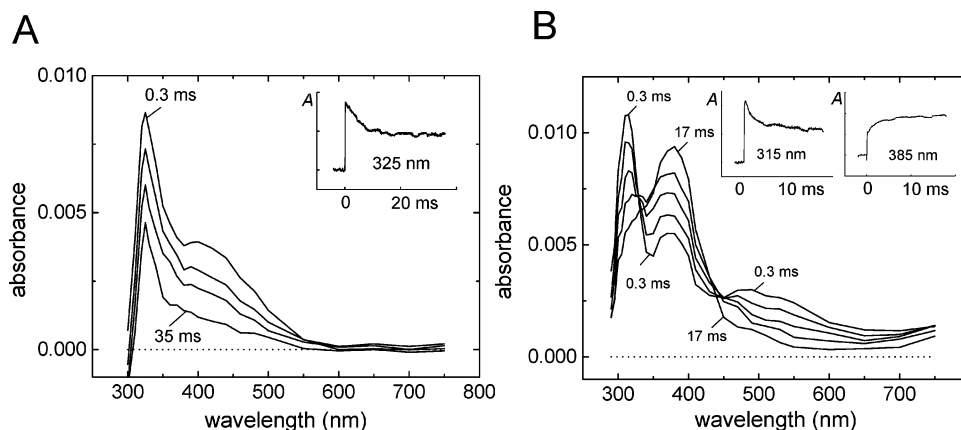(28) Adam, W.; Saha-Moeller, C. R.; Schoenberger, A. *J. Am. Chem. Soc.* **1996**, *118*, 9233−9238.
(29) Martinez, G. R.; Medeiros, M. H.; Ravanat, J. L.; Cadet, J.; Di Mascio, P. *Biol. Chem.* **2002**, *383*, 607−617.
(30) Adam, W.; Arnold, M. A.; Grune, M.; Nau, W. M.; Pischel, U.; Saha-Moeller, C. R. *Org. Lett.* **2002**, *4*, 537−540.
(31) Lymar, S. V.; Schwarz, H. A.; Czapski, G. *J. Phys. Chem. A* **2002**, *106*.

(32) Candeias, L. P.; Steenken, S. *J. Am. Chem. Soc.* **1989**, *111*, 1094−1099.

Figure 2. Transient absorption spectra of the oligonucleotides 5′-d(CC[2AP]TC**X**CTACC) in the single-stranded forms. (A) X = 8-oxoGua and (B) X = G. The spectra were recorded at various delay times after photoexcitation of the single-stranded (50 μM) oligonucleotides with the actinic 308 nm laser flashes (60 mJ/pulse/cm², 1 pulse/s) in deoxygenated 5 mM phosphate buffer solution (pH 7.5) containing 1 mM NaNO₃ and 100 mM NaCl. The insets show the transient absorption profiles recorded at the representative wavelengths.

deprotonation of the G•⁺ radical cation is very fast and the lifetime of G•⁺ does not exceed 300 ns.[36] The absorbance of •NO₂ radicals is expected to be very weak due to the negligible molar absorptivities of •NO₂ in this spectral range[31] and thus cannot be directly observed in these experiments. The amplitudes of the 8-oxoGua(−H)• and G(−H)• absorbance signals in the case of duplexes **1** and **2** (data not shown) were significantly lower than those in the single-stranded oligonucleotides 5′-d(CC-[2AP]TC**X**CTACC) (Figure 2). This difference in signal amplitudes is in agreement with a lower efficiency of two-photon ionization of 2AP in double-stranded than in single-stranded oligonucleotides.[12,26,37]

A decrease in temperature does not result in any observable effect on the yields of 8-oxoGua(−H)• radicals. Indeed, the initial 325 nm amplitudes of the 8-oxoGua(−H)• signals recorded at 9 °C or at room temperature were similar in both single- and double-stranded oligonucleotides. At 9 °C, the signals of 8-oxoGua(−H)• in duplex **1** with the normal complementary strand were close to those in duplex **3** with the shorter complementary strand. This observation is a further indication that the dissociation of duplex **3** is negligible at 9 °C. In single-stranded oligonucleotides, the photoionization of 2AP is more efficient than that in duplexes and the yield of 8-oxoGua(−H)• radicals would have higher if dissociation of duplex **3** had occurred.[12,26,37]

In the presence of •NO₂ radicals, the fates of 8-oxoGua(−H)• and G(−H)• radicals are quite different (Figure 2). The decay of the G(−H)• transient absorption at 315 nm is associated with the appearance of a characteristic absorption band of the nitro group at 385 nm (Figure 2B).[19−25] The nitro adducts formed are stable and can be isolated by reversed-phase HPLC. In agreement with previous observations,[24,25] we found that these products are 5-guanidino-4-nitroimidazole and 8-nitroguanine formed with relative yields of ∼70% and ∼30%, respectively. Using the ratio of the signal amplitudes at 315 and 385 nm (Figure 2A) and the molar absorptivities of dG(−H)• (ϵ_{315} =

7.3 × 10³ M⁻¹ cm⁻¹),[9] NIm (ϵ_{385} = 6.6 × 10³ M⁻¹ cm⁻¹), and 8-nitroGua (ϵ_{385} = 8.4 × 10³ M⁻¹ cm⁻¹),[25] we estimated that the yield of nitro products is close to quantitative (80−90%). The observation of an isosbestic point around 330 nm in the transient absorption spectra (Figure 2B) confirms that the dG-(−H)• radical is transformed predominantly to nitration products. Thus, formation of the nitro end-products is the major pathway of reaction of G(−H)• radicals with •NO₂.

In contrast, the decay of 8-oxoGua(−H)• radicals results only in a gradual reduction of the 8-oxoGua(−H)• transient absorption without the appearance of a new absorption band (Figure 2A). These observations indicate that oxidation rather than nitration is the dominant mode of the combination reaction of 8-oxoGua-(−H)• with •NO₂.

Kinetics of Radical Combination. The decay of the 8-oxo-Gua(−H)• and G(−H)• absorption bands (Figure 2, insets) were assigned to the combination of •NO₂ with 8-oxoGua(−H)• (reaction 1) or with G(−H)• (reaction 2) radicals (Table 1). The kinetics of these reactions can be described by the following equation, obtained by the integration of the differential equation describing the second-order kinetics

$$A_t = (A_0 - A_\infty)/[1 + A_0(k_1/\epsilon_R)t] + A_\infty \qquad (1)$$

where, A_0 is the absorbance determined just after the end of actinic laser flash, A_∞ is the final absorbance, and ϵ_R denotes the molar absorptivities of 8-oxoGua(−H)• (11.3 × 10³ M⁻¹ cm⁻¹ at 325 nm)[9] and G(−H)• (7.3 × 10³ M⁻¹ cm⁻¹ at 315 nm).[10] The rate constants were calculated by fitting eq 1 to the transient absorption profiles. Table 1 shows that the combination reaction of •NO₂ radicals with 8-oxoGua(−H)• and G(−H)• radicals occurs with similar rates in both single- and double-stranded oligonucleotides. Therefore, differences in the reduction potentials of the radicals, as well as the DNA secondary structure, exert only small effects on the combination rates. Under our experimental conditions (equal initial concentrations of •NO₂ and 8-oxoGua(−H)• or G(−H)• radicals), the contributions of the side reactions 4 and 5 (Table 1) of •NO₂ radicals are relatively small.[38]

Indeed, the establishment of equilibrium between •NO₂ and N₂O₄ species is faster than the rate of dissociation of N₂O₄ ($k_{−4}$

(33) Stemp, E. D. A.; Arkin, M. R.; Barton, J. K. *J. Am. Chem. Soc.* **1997**, *119*, 2921−2925.
(34) Stemp, E. D. A.; Barton, J. K. *Inorg. Chem.* **2000**, *39*, 3868−3874.
(35) Dohno, C.; Stemp, E. D. A.; Barton, J. K. *J. Am. Chem. Soc.* **2003**, *125*, 9586−9587.
(36) Kobayashi, K.; Tagawa, S. *J. Am. Chem. Soc.* **2003**, *125*, 10213−10218.
(37) Shafirovich, V.; Dourandin, A.; Huang, W.; Luneva, N. P.; Geacintov, N. E. *Phys. Chem. Chem. Phys.* **2000**, *2*, 4399−4408.

(38) Neta, P.; Huie, R. E.; Ross, A. B. *J. Phys. Chem. Ref. Data* **1988**, *17*, 1027−1284.

Table 1. Kinetic Parameters of Combination of $^{\bullet}NO_2$ Radicals with 8-oxoGua(−H)$^{\bullet}$ and G(−H)$^{\bullet}$ Radicals in DNA

N	Reaction	k_n, M⁻¹s⁻¹	ref.
1	5'-CC[2AP]TC[**8-oxoGua(-H)$^{\bullet}$**]CTACC + $^{\bullet}NO_2$ → products	$(4.3\pm0.5)\times10^{8\ a}$	this work
	5'-CC[2AP]TC[**8-oxoGua(-H)$^{\bullet}$**]CTACC 3'-GG---T--AG-------C----------GATGG $\quad$ + $^{\bullet}NO_2$ → products	$(4.2\pm0.8)\times10^{8\ a}$	this work
2	5'-CC[2AP]TC[**G(-H)$^{\bullet}$**]CTACC + $^{\bullet}NO_2$ → products	$(4.5\pm0.5)\times10^{8\ a,b}$	this work
	5'-CC[2AP]TC[**G(-H)$^{\bullet}$**]CTACC 3'-GG---T--AG---C-----GATGG $\quad$ + $^{\bullet}NO_2$ → products	$(4.3\pm0.8)\times10^{8\ a}$	this work
3	$e^- + NO_3^- \rightarrow\ ^{\bullet}NO_2$	1.9×10^{10}	13
4	$^{\bullet}NO_2 + ^{\bullet}NO_2 \rightarrow N_2O_4$	4.5×10^8	38
−4	$N_2O_4 \rightarrow\ ^{\bullet}NO_2 + ^{\bullet}NO_2$	$6.9\times10^3\ s^{-1}$	38
5	$N_2O_4 + H_2O \rightarrow NO_2^- + NO_3^- + 2H^+$	$1\times10^3\ s^{-1}$	38

[a] The rate constants were measured in deoxygenated buffer solutions containing 1 mM NaNO₃ and 100 mM NaCl, and uncertainties are given as standard errors for the best least-squares fits of the appropriate kinetic equations to the transient absorption profiles of 8-oxoGua(−H)$^{\bullet}$ and G(−H)$^{\bullet}$ radicals recorded at 325 and 315 nm, respectively. [b] The values of k_2 obtained from the growth of the nitro group absorption at 385 nm were the same as those measured at 315 nm within the experimental accuracy.
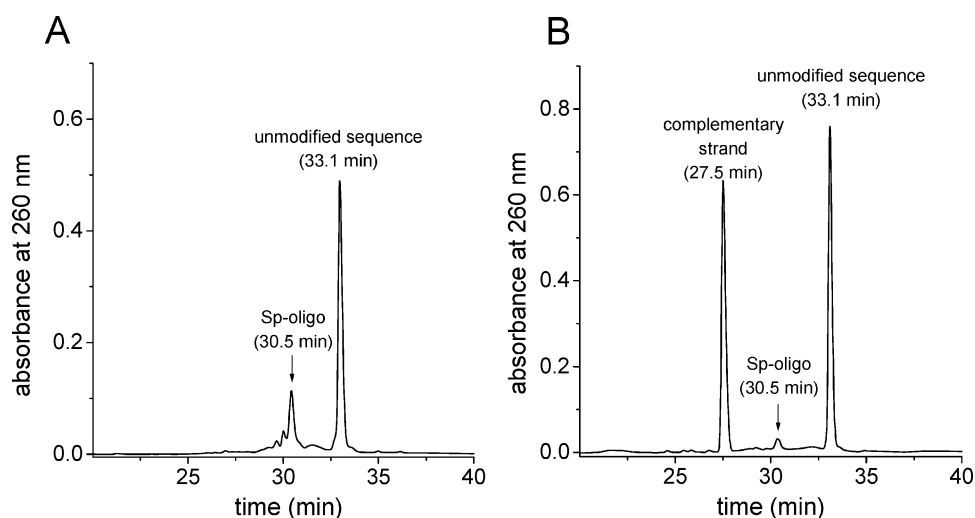

Figure 3. Reversed-phase HPLC elution profiles of 8-oxoGua oxidation products. The 25 μM sample solutions of (A) the single-stranded 5′-d(CC[2AP]-TC[**8-oxoGua**]CTACC) sequence or (B) the 5′-d(CC[2AP]TC[**8-oxoGua**]CTACC)·5′-d(GCGTAG) duplex in deoxygenated 5 mM phosphate buffer solution (pH 7.5) containing 1 mM NaNO₃ and 100 mM NaCl were excited by a train of 308 nm XeCl excimer laser pulses (60 mJ/pulse/cm², 10 pulse/s) at 9 °C for 4 or 8 s, respectively. HPLC elution conditions (detection of products at 260 nm): 8−20% linear gradient of acetonitrile in 50 mM triethylammonium acetate (pH 7) for 60 min at a flow rate of 1 mL/min. The unmodified sequence 5′-d(CC[2AP]TC[**8-oxoGua**]CTACC) elutes at 33.1 min, the same oligonucleotide but with a spiroiminodihydantoin lesion replacing 8-oxoGua at 30.5 min, and the complementary strand 5′-d(GCGTAG) at 27.5 min.

$> k_5$), and the rate constant of $^{\bullet}NO_2$ decay in such side reactions (4 and 5) can be estimated as $k_{4,5} \approx (k_4/k_{-4})k_5 \approx 7\times10^7$ M⁻¹ s⁻¹. These estimates demonstrate that the contribution of the reactions 4 and 5 do not exceed ∼15% of the overall decay pathways of $^{\bullet}NO_2$ dominated by reactions 1 or 2. This is close to the standard error in our measurements (Table 1). The contributions of potential reactions of N₂O₄ species (that frequently yield the same products as $^{\bullet}NO_2$)[39] with 8-oxoGua-(−H)$^{\bullet}$ and G(−H)$^{\bullet}$ radicals are thus expected to be small. Under our experimental conditions (∼1 μM concentrations of radical species), equilibrium between $^{\bullet}NO_2$ and N₂O₄ species is shifted toward the formation of $^{\bullet}NO_2$ ($k_{-4} > k_4[^{\bullet}NO_2]$). Thus, the rate constants of reaction of N₂O₄ with 8-oxoGua(−H)$^{\bullet}$ and G(−H)$^{\bullet}$ radicals should be at least 1 order of magnitude greater than k_1 and k_2 to compete with reactions 1 and 2.

End-Products of Oxidation and Nitration Reactions. The oxidation products generated by the irradiation of the single-stranded oligonucleotide 5′-d(CC[2AP]TC[**8-oxoGua**]CTACC) with 308 nm laser pulses in deoxygenated buffer solutions (pH 7.5) containing 1 mM NaNO₃ were separated by reversed-phase HPLC methods (Figure 3A). The unmodified oligonucleotide elutes at 33.1 min, and the prominent reaction product eluting as a narrow peak is observed at 30.5 min. The MALDI-TOF mass spectrum of the 30.5 min fraction recorded in the negative mode exhibits a major signal at m/z 3268.2 (Figure 4A), whereas the unmodified sequence shows a signal at m/z 3252.2 (M). This oxidized oligonucleotide has a mass of M + 16 that characterizes the spiroiminodihydantoin product of 8-oxoGua oxidation,[14−18] initially designated as 4-hydroxy-7,8-dihydro-7,8-oxo-guanine.[27,28]

The formation of the Sp lesions was further verified by digesting the Sp modified oligonucleotides to the nucleobase

(39) Huie, R. E. *Toxicology* **1994**, *89*, 193−216.
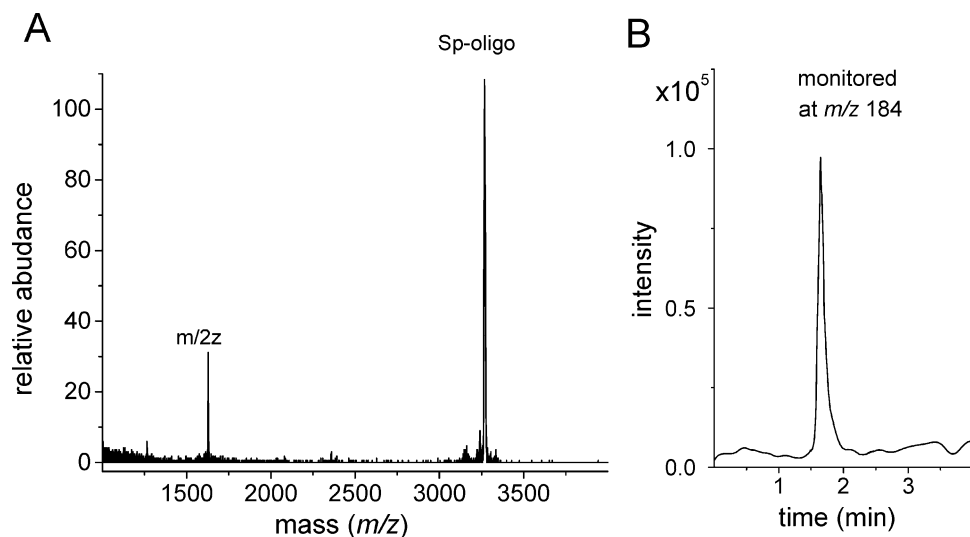
Figure 4. Identification of 8-oxoGua oxidation products. MALDI-TOF negative ion spectrum (A) of the 5′-d(CC[2AP]TC[**Sp**]CTACC oligonucleotide isolated by reversed-phase HPLC using the same conditions as in Figure 3 and purified by a second HPLC cycle. Extracted chromatogram (B) of the spiroiminodihydantoin nucleobase obtained after the chemical hydrolysis of the Sp adduct with hydrogen fluoride in pyridine.[27] This chromatogram was recorded in the positive mode with specific ion monitoring at m/z 184.

level and coeluting the Sp obtained with an authentic Sp standard. Previous experiments showed that the treatment of the oligonucleotides containing the Sp lesions by endonucleases (nuclease P1) and exonucleases (snake venom phosphodiesterase I and calf spleen phosphodiesterase II) resulted in incomplete digestions.[18] In agreement with the results of Cadet and co-workers,[40] we found that the phosphodiester bond between the Sp and the 5′-flanking nucleoside is resistant to hydrolysis by phosphodiesterases II.[18] Therefore, in this work we employed a "soft" chemical hydrolysis method utilizing hydrogen fluoride stabilized in pyridine to hydrolyze the Sp oligonucleotide to the nucleobase level thus quantitatively releasing the pair of diastereomeric Sp bases.[27] Again utilizing the HPLC-ESI/MS method, a prominent peak due to the Sp nucleobase is evident in the positive mode with specific ion monitoring at $m/z = 184$ (Figure 4B). The identity of the Sp nucleobases derived from the chemical hydrolysis of the oligonucleotides was further verified by coelution of the oxidation products of 8-oxoGua with the authentic Sp nucleobase standards (data not shown) obtained by the chemical hydrolysis of the Sp nucleoside standards.[27]

Oxidation of the 8-oxoGua residues in the double-stranded form was explored using the duplex **2** with the short complementary strand, 5′-d(GCGTAG), that does not interfere with the separation of the oxidized strand 5′-d(CC[2AP]TC[**8-oxoGua**]CTACC) during the course of reversed-phase HPLC analysis (Figure 3B). To prevent the dissociation of the double-stranded form during the laser irradiation, the sample solutions of the duplex **2** were photoirradiated at 9 °C. Typical HPLC elution profiles obtained after a 10 s laser excitation of duplex **2** in deoxygenated buffer solution (pH 7.5) exhibit three peaks. The complementary 6-mer strand and the unmodified 11-mer oligonucleotide elute at 27.5 and 33.1 min, respectively, and the third fraction with Sp substituting for 8-oxoGua in the 11-mer, elutes at 30.5 min. This modified oligonucleotide eluted with the same retention time and exhibited the same MALDI-

(40) Romieu, A.; Gasparutto, D.; Molko, D.; Ravanat, J.-L.; Cadet, J. *Eur. J. Org. Chem.* **1984**, *49*, 9−56.
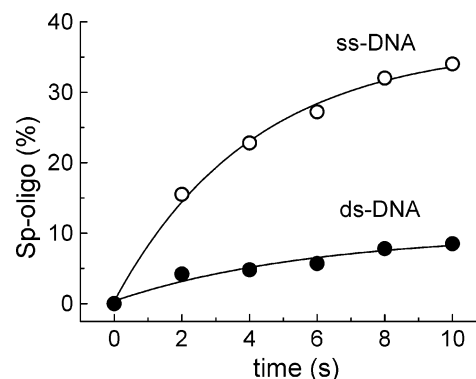
Figure 5. Time dependent yields of the Sp lesions in (A) single-stranded and (B) double-stranded oligonucleotides. The oligonucleotide samples (25 μM) were excited using the same conditions as those in Figure 3. The yields of the Sp lesions were calculated by integration of the HPLC elution patterns.

TOF signal at m/z 3268.2 as the adduct derived from the irradiation and oxidation of the single-stranded 5′-d(CC[2AP]-TC[**8-oxoGua**]CTACC)sequence.

The dynamics of oxidative damage initiated by intense 308 nm laser pulse excitation was studied at 9 °C. At this temperature, the dissociation of duplex **3** is negligible and the dynamics of Sp formation can be compared with that in the single-stranded sequence also at 9 °C. It is shown in Figure 5 that the yield of Sp (expressed as a percentage of the initial oligonucleotide starting concentration) increases as a function of irradiation time.

In the single-stranded sequence, the yields of Sp attain maximum levels of ∼30−35% (similar to those observed at room temperature) after a 8−10 s exposure of the solution to the 10 pulse/s laser pulse train. In the case of duplex **3**, the observations are similar except that the buildup of the Sp yields is slower (Figure 5). This is in agreement with the lower efficiency of two-photon photoionization of 2AP in double-stranded DNA[12,26,37] that results in a less efficient generation of the 8-oxoGua(−H)•, and thus •NO₂ radicals, in double-stranded DNA.

The nitro adducts generated by irradiation of the single-stranded oligonucleotide 5′-d(CC[2AP]TCGCTACC) with 308

Table 2. Kinetic Parameters of NO_2^- Oxidation by $G(-H)^\bullet$ Radicals and Oxidation of 8-oxoGua with $^\bullet NO_2$ Radicals in DNA

N	reaction	k_n, M^{-1} s^{-1}	ref
6	5′-CC[2AP]TC[**G(−H)**$^\bullet$]CTACC + NO_2^- → products	$(1.0 \pm 0.2) \times 10^{6a}$	this work
7	dGMP(−H)$^\bullet$ + NO_2^- → products	2.6×10^6	11
8	e^- + N_2O + H^+ → $^\bullet OH$ + N_2	9.1×10^9	13
9	$^\bullet OH$ + $(CH_3)_3COH$ → H_2O + $^\bullet CH_2C(CH_3)_2OH$	6×10^8	13
10	e^- + NO_2^- + $2H^+$ → $^\bullet NO$ + H_2O	4×10^9	13
11	5′-CCATC[**8-oxoGua**]CTACC + $^\bullet NO_2$ → 5′-CCAT[**8-oxoGua(−H)**$^\bullet$]CTACC + NO_2^-	$(8 \pm 2) \times 10^{5b}$	this work
12	5′-CCATC[8-oxoGua]CTACC + $SO_4^{\bullet-}$ → products	$\sim 6 \times 10^{9c}$	this work
13	8-oxodGuo + $^\bullet NO_2$ → 8-oxodGuo(−H)$^\bullet$ + NO_2^-	5.3×10^6	11
14	$S_2O_8^{2-}$ + $h\nu$ → $2SO_4^{\bullet-}$	$\varphi_{308} = 0.55$	43
15	$SO_4^{\bullet-}$ + NO_2^- → SO_4^{2-} + $^\bullet NO_2$	8.8×10^8	38

^{a} Measured in buffer solutions containing 0.5 M *tert*-butyl alcohol and 100 mM NaCl. ^{b} Obtained by numeric analysis of the kinetic traces of the growth of the 8-oxoGua(−H)$^\bullet$ absorption. ^{c} Estimated from the decay of $SO_4^{\bullet-}$ radicals at 445 nm.

nm laser pulses in deoxygenated buffer solutions (pH 7.5) containing 1 mM $NaNO_3$ were separated by reversed-phase HPLC. In agreement with previous observations,[24,25] the NIm adduct elutes as a narrow prominent peak before the unmodified sequence, whereas the 8-nitroGua adduct elutes after the unmodified sequence (data not shown). The relative yields of the NIm (~70%) and 8-nitroGua (~30%) adducts calculated from the chromatogram (detection at 385 nm) were very close to the yields reported earlier.[24,25] The MALDI-TOF mass spectra of these adducts recorded in the negative mode exhibit a unique series of ions associated with the intact adducts and the nitroso and amino derivatives. The latter products arise from the fragmentation of the nitro groups induced by the intense UV laser pulses that vaporize the sample in the MALDI-TOF mass spectrometer as described in detail previously.[24,25] To summarize, the NIm adduct was identified by the major signal of the intact adduct (*m/z* 3255.1, M + 19) and two minor peaks of the nitroso (*m/z* 3239.2, M + 3) and amino (*m/z* 3224.2, M − 11) derivatives as described in details elsewhere.[24,25] In the case of the 8-nitroGua adduct, fragmentation of the nitro group is more efficient and the major peak is attributed to the nitroso derivative (*m/z* 3266.9, M + 29); the intact adduct (M + 45) and the amino (M + 15) derivative were identified by the minor signals at *m/z* 3282.3 and *m/z* 3252.0, respectively. The identity of the NIm and 8-nitroGua adducts was confirmed by coelution with the authentic oligonucleotide standards synthesized as described before.[24,25]

Oxygen-18 Isotope Labeling. More insights into the mechanistic aspects of 8-oxoGua oxidation by $^\bullet NO_2$ radicals and the mechanisms of formation of Sp lesions were obtained by performing photooxidation experiments in $H_2^{18}O$ buffer solutions. In these experiments the 5′-d(CC[2AP]TC[**8-oxoGua**]CTACC) sequence was irradiated in deoxygenated $H_2^{18}O$ buffer solutions, and the free base spiroiminodihydantoin, obtained by chemical hydrolysis of the Sp adduct with hydrogen fluoride in pyridine,[27] was subjected to HPLC-ESI/MS analysis.

The extracted chromatogram recorded in the positive mode with the specific ion monitoring at *m/z* 186 shows a prominent peak corresponding to the Sp free base containing one ^{18}O atom from $H_2^{18}O$ (Figure 6). In contrast, this sample does not contain the normal Sp base with two ^{16}O atoms detected at *m/z* 184. Thus, these experiments indicate that the additional O-atom in Sp originates from $H_2^{18}O$, not from $^\bullet N^{16}O_2$ radicals that are derived from the reduction of $N^{16}O_3^-$ anions by hydrated electrons.
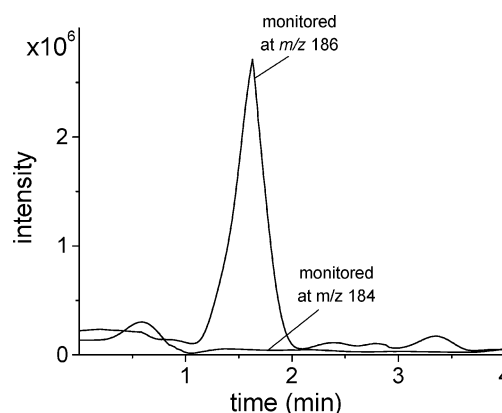
Figure 6. HPLC-ESI/MS analysis of spiroiminodihydantoin in the free base form. The extracted chromatograms were recorded in the positive mode with specific ion monitoring at *m/z* 184 and 186. The Sp adduct was prepared by photoexitation of the 5′-d(CC[2AP]TC[**8-oxoGua**]CTACC) sequence in $H_2^{18}O$ buffer solution, isolated by reversed-phase HPLC using the same conditions as those in Figure 3 and digested by chemical hydrolysis with hydrogen fluoride in pyridine.[27]

Redox Cycling of $^\bullet NO_2/NO_2^-$. The reduction potential of $^\bullet NO_2$,[8] E° = 1.04 V vs NHE, is greater than the midpoint oxidation potential of 8-oxodGuo,[9] E_7 = 0.74 V vs NHE, but less than that of dG,[10] E_7 = 1.29 V vs NHE. Therefore, $G(-H)^\bullet$ radicals produced by oxidizing agents ($^\bullet OH$ or $CO_3^{\bullet-}$) or ionizing radiation in cellular environments can be repaired by reactions with NO_2^- anions, and in turn, $^\bullet NO_2$ radicals derived from these reaction can selectively oxidize 8-oxoGuo. Indeed, our laser flash photolysis experiments showed that free base dGMP(−H)$^\bullet$ radicals oxidize NO_2^- anions, whereas $^\bullet NO_2$ radicals oxidize 8-oxodGuo.[11] In this work we explore the redox cycling of the $^\bullet NO_2/NO_2^-$ species using oligonucleotides.

In the NO_2^- oxidation experiments (reaction 6, Table 2), $G(-H)^\bullet$ radicals were generated in buffer solutions of the 5′-d(CC[2AP]TC**G**CTACC) sequence saturated with nitrous oxide that rapidly traps the hydrated electrons (reaction 8) and thus prevents the reduction of NO_2^- (reaction 10 in Table 2). Hydroxyl radicals produced in reaction 8 (Table 2) were trapped by *tert*-butyl alcohol (reaction 9) that was also added to the reaction mixture. The $^\bullet CH_2C(CH_3)_2OH$ radicals formed in this reaction are relatively inert.[41] In agreement with our previous results,[42] the $G(-H)^\bullet$ radicals in the 5′-d(CC[2AP]TC**G**CTACC)

(41) Flyunt, R.; Leitzke, A.; Mark, G.; Mvula, E.; Reisz, E.; Schick, R.; von Sonntag, C. *J. Phys. Chem. B* **2003**, *107*, 7242−7253.
(42) Misiaszek, R.; Crean, C.; Joffe, A.; Geacintov, N. E.; Shafirovich, V. *J. Biol. Chem.* **2004**, *279*, 32106−32115.

A

B
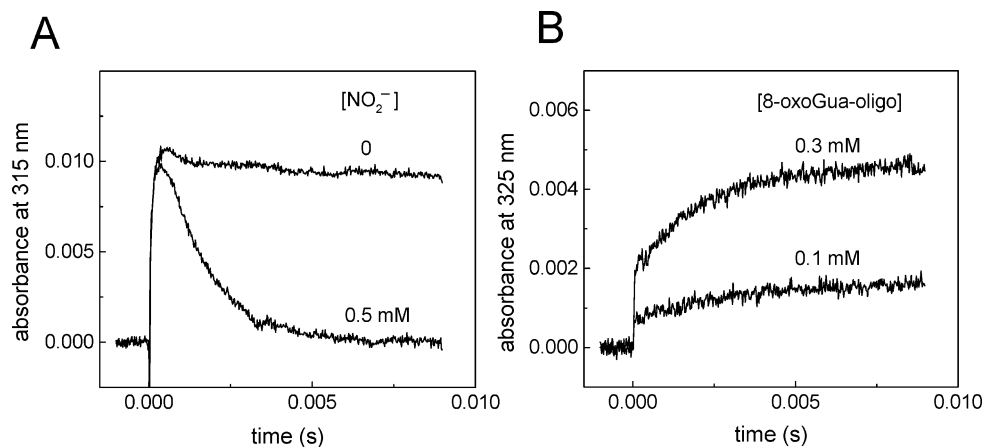
Figure 7. (Panel A) Kinetics of the decay of G(−H)• radicals in the absence and presence of NO₂⁻. The 5′-d(CC[2AP]TC**G**CTACC) samples were dissolved in 5 mM phosphate buffer solution (pH 7.5) containing 100 mM NaCl, 0.5 M *tert*-butyl alcohol, and 0 or 0.5 mM NaNO₂, and the solutions were saturated with N₂O. (Panel B) Kinetics of 8-oxoGua oxidation in the oiligonucleotide 5′-d(CCATC[**8-oxoGua**]CTACC) by •NO₂ radicals monitored by the absorbance of the 8-oxoGua(−H)• radicals at 325 nm. The samples dissolved in 5 mM sodium phosphate buffer solution (pH 7.5) containing 4 mM N₂S₂O₈ and 10 mM NaNO₂ were deoxygenated with argon. The solutions were photoexcited using the same conditions as those in Figure 2.

sequence are stable and do not decay significantly on a millisecond time scale (Figure 7A).

A similar approach has been extensively exploited in studies of guanine radical reactions by pulse radiolysis techniques.[10,44,45] Addition of NO₂⁻ anions at a 0.5 mM concentration significantly reduces the lifetime of G(−H)• radicals (Figure 7A). At $[NO_2^-] > [G(−H)•]$, the decay of G(−H)• is described by pseudo-first-order kinetics with an observed rate constant, k_6'. The value of k_6' increases linearly with the concentration of NO₂⁻ anions (see, for more details, Supporting Information) according to the following equation:

$$k_6' = 1/\tau_0 + k_6[NO_2^-] \qquad (2)$$

where τ_0 is the lifetime of the G(−H)• radicals in the absence of NO₂⁻ anions. The value of k_6 calculated from the slope of the k_6' vs [NO₂⁻] plot is smaller by a factor of 2.6 than the k_7 value for the oxidation of NO₂⁻ by the free base dGMP(−H)• radicals (reaction 7, Table 2). The HPLC analysis of the photooxidation products showed a significant decrease in the oligonucleotide degradation rates and the absence of the nitration products (data not shown).

The 5′-d(CCATC[**8-oxoGua**]CTACC) sequence was used to explore the oxidation of 8-oxoGua by •NO₂ radicals (reaction 11, Table 2) that are generated by the oxidation of NO₂⁻ by SO₄•⁻ radicals (reaction 15). The latter radicals were generated by the selective photochemically induced dissociation of S₂O₈²⁻ anions with 308 nm excimer laser pulses (reaction 14).[43] The initial concentrations of S₂O₈²⁻ anions were adjusted to obtain a ∼1 μM SO₄•⁻ concentration after a single laser shot. The growth of the characteristic absorption of 8-oxoGua(−H)• at 325 nm exhibits two components (Figure 7B). The prompt component rising within less than 1 μs is due to oxidation of 8-oxoGua by SO₄•⁻ radicals (reaction 12). The amplitude of this signal increases with the concentration of the 8-oxoGua-containing oligonucleotides due to competition of reactions 12 and 15. The second component shows the slower growth of the 8-oxoGua(−H)• absorption attributed to oxidation of 8-oxoGua

by •NO₂ radicals (reaction 11). Although, the contribution of the side reactions 4 and 5 (Table 1) of •NO₂ radicals is relatively small, yields of 8-oxoGua(−H)• calculated from Figure 7B do not exceed ∼40% relative to initial radical concentrations after a laser flash (∼1 μM). The low efficiency of 8-oxoGua(−H)• formation is an indication of the competitive trapping of •NO₂ radicals by 8-oxoGua (reaction 11, Table 2) and by 8-oxoGua-(−H)• (reaction 1, Table 1). The rate constant of 8-oxoGua oxidation by •NO₂ radicals was obtained from a numerical analysis of the transient absorption profiles of 8-oxoGua(−H)• formation using the PRKIN program developed by H. Schwarz at the Brookhaven National Laboratory (see, for more details Supporting Information). The value of k_{11} is by a factor of 6.6 smaller than the k_{12} value for the oxidation of free base 8-oxodGuo (reaction 12, Table 2). Using a combination of HPLC and MALDI-TOF methods we found that the major products of 8-oxoGua oxidation are the Sp lesions (data not shown).

Thus, these experiments show that G(−H)• radicals within the oligonucleotide oxidize NO₂⁻ anions, and in turn •NO₂ radicals produce 8-oxoGua(−H)• radicals in the 8-oxoGua oligonucleotide. The rate constants of these reactions are smaller by a factor of 2.6−6.6 than those for free nucleosides (Table 2).

Discussion

Interplay of Oxidation and Nitration: Mechanistic Aspects. The direct spectroscopic time-resolved measurements described here demonstrate that the fates of 8-oxoGua(−H)• and G(−H)• radicals in reactions with •NO₂ radicals are quite different. The combination reaction of 8-oxoGua(−H)• and •NO₂ radicals does not give rise to the appearance of the characteristic UV absorption spectrum of the nitro products (Figure 2A) and, instead, results in the formation of oxidative modifications of 8-oxoGua residues, the spiroiminodihydantoin lesions.[14−18] The Sp adducts were isolated by reversed-phase HPLC methods (Figure 3) and identified by MALDI-TOF/MS and HPLC-ESI/MS analysis (Figure 4). In contrast, the combination of G(−H)• and •NO₂ radicals is associated with the growth of an absorption band in the spectral range 320−450 nm due to the nitro group (Figure 2B), and the nitro end-

(43) Ivanov, K. L.; Glebov, E. M.; Plyusnin, V. F.; Ivanov, Y. V.; Grivin, V. P.; Bazhin, N. M. *J. Photochem. Photobiol. A* **2000**, *133*, 99−104.
(44) Steenken, S. *Chem. Rev.* **1989**, *89*, 503−520.
(45) Steenken, S. *Biol. Chem.* **1997**, *378*, 1293−1297.
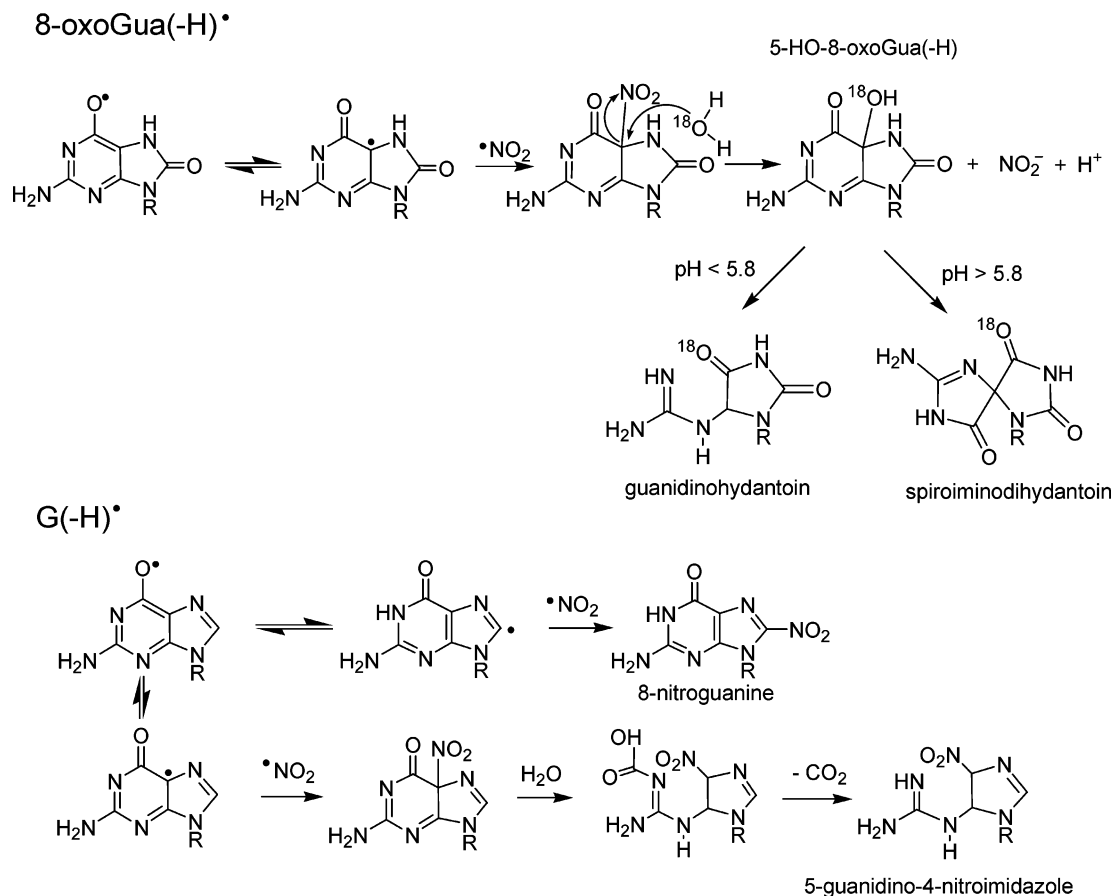
Figure 8. Formation of oxidation and nitration products via the combination reaction of •NO₂ with 8-oxoGua(−H)• and G(−H)• in DNA.

products NIm and 8-nitroGua adducts are found as previously described.[24,25] The rate constants of the radical combination reactions of •NO₂ radicals with 8-oxoGua(−H)• and G(−H)• radicals are very close to one another and do not depend on the DNA secondary structure (Table 1). These observations can be explained in terms of the scheme shown in Figure 8. According to this mechanism, the first step is the formation of the adduct between the •NO₂ radical and either the 8-oxoGua(−H)• or the G(−H)• radicals. In the •NO₂ radical, the unpaired electron is delocalized on the N and the O atoms[46] and, in principle, both N and O atoms can participate in the formation of chemical bonds with another target radical. Here, we propose that the formation of •NO₂ with an 8-oxoGua(−H)• or G(−H)• radical results in the formation of a nitrogen−carbon bond.

The G(−H)• radicals are usually considered to be O-centered radicals with the unpaired electron positioned on the O6 atom,[47,48] which explains the low reactivity of this radical with molecular oxygen.[42,49] However, formation of a covalent bond between radicals depends on the stabilities of the adducts formed rather than on the spin densities on particular atoms. Here, addition of •NO₂ radicals to the C8 or C5 positions of a G(−H)• radical leads to a stable 8-nitroGua lesion and an unstable 5-nitroGua intermediate that spontaneously collapses to the stable NIm derivative (Figure 8). The relative yields of

the NIm (∼70%) and 8-nitroGua (∼30%) lesions obtained here are very close to the yields reported previously where G(−H)• radicals were derived from the one-electron oxidation of guanine residues by carbonate radical anions.[24,25] These observations demonstrate that the ratio of the NIm and 8-nitroGua lesions is determined by the addition of •NO₂ radicals either to the C5 or to the C8 positions of the G(−H)• radical and does not depend on the method of generation of the G(−H)• radical.

In the case of 8-oxoGua(−H)• radicals, the C5 nitro adduct formed is unstable. We propose that the hydrolysis of this adduct occurs via nucleophilic addition of water molecule to C5 followed by release of the NO₂⁻ anion and formation of the 5-HO-8-oxoGua(−H) intermediate (Figure 8).

According to this mechanism the 5-HO-8-oxoGua(−H) adduct contains the O-atom from H₂¹⁸O (not from N¹⁶O₂). The subsequent transformation of the 5-HO-8-oxoGua(−H) adduct depends on the solution pH and results in the formation of either spiroiminodihydantoin or guanidinohydantoin (Gh) lesions.[14−18,50,51] Tannenbaum et al. proposed that the partitioning of 5-HO-8-oxoGua(−H) into either Sp or Gh is determined by different reactivities of the deprotonated and protonated forms of this adduct (pK_a ≈ 5.8).[51] Decreasing pH < 5.8 favors pyrimidine ring opening, followed by the formation of the Gh lesions; in contrast, the acyl shift leading to the Sp lesions dominates at pH > 5.8. The proposed mechanism (Figure 8) explains two important observations: (*i*) the combination of

(46) Behar, D.; Fessenden, R. W. *J. Phys. Chem.* **1972**, *76*, 1710−1721.
(47) Hildenbrand, K.; Schulte-Frohlinde, D. *Free Radical Res. Commun.* **1990**, *11*, 195−206.
(48) Schiemann, O.; Turro, N. J.; Barton, J. K. *J. Phys. Chem. B* **2000**, *104*, 7214−7220.
(49) Shafirovich, V.; Dourandin, A.; Huang, W.; Geacintov, N. E. *J. Biol. Chem.* **2001**, *276*, 24621−24626.

(50) Luo, W.; Muller, J. G.; Rachlin, E. M.; Burrows, C. J. *Chem. Res. Toxicol.* **2001**, *14*, 927−938.
(51) Niles, J. C.; Wishnok, J. S.; Tannenbaum, S. R. *Chem. Res. Toxicol.* **2004**, *17*, 1510−1519.

•NO$_2$ and 8-oxoGua(−H)• radicals occurs with a rate constant typical for radical−radical addition reactions (Table 1), and (*ii*) the O-atom in the oxidation product formed originates from water (Figure 6). An alternative mechanism is electron transfer from 8-oxoGua(−H)• to •NO$_2$ with the formation of the intermediate 8-oxoGua(−H)$^+$ cation and NO$_2^-$ anion. Addition of H$_2$^{18}O to 8-oxoGua(−H)$^+$ cation proposed by Burrows et al. in the course of 8-oxoGua oxidation by IrCl$_6^{4-}$ leads to the 5-HO-8-oxoGua(−H) precursor of the Gh and Sp lesions containing the ^{18}O-isotope from a water molecule.[14,52] However, such an electron transfer mechanism cannot explain the high rate constants for the combination reaction measured here experimentally (Table 1). The electron-transfer reactions of •NO$_2$ radicals are typically slow due to a small self-exchange rate constant and a high internal reorganization energy in the •NO$_2$/NO$_2^-$ system.[53] These factors account for the lower reactivity of •NO$_2$ radicals in bimolecular outersphere electron-transfer reactions in comparison with typical electron acceptors, such as aromatic radical cations.[11]

Biological Implications. The •NO$_2$ radical is an important biological intermediate that is ubiquitous in living systems.[7] In vivo, •NO$_2$ radicals, the products of normal metabolic activity, are rapidly deactivated by antioxidants that reduce the •NO$_2$ radicals to nitrite anions. However, in tissues subjected to chronic infection and inflammation, •NO$_2$ radicals are overproduced via the activation of neutrophils and macrophages.[3] In neutrophils, formation of •NO$_2$ radicals involves the enzymatic oxidation of NO$_2^-$ anions by hydrogen peroxide catalyzed by myeloperoxidases. Activation of macrophages results in over-production of •NO and superoxide radicals that combine to form the toxic compound peroxynitrite.[54] Homolysis of peroxynitrite can occur spontaneously or catalytically with the participation of carbon dioxide[55,56] and is another important pathway of formation of •NO$_2$ in vivo.[57,58] Due to its mild reduction potential ($E°$ = 1.04 V vs NHE),[8] the •NO$_2$ radical does not exhibit observable reactivities with any of the normal nucleobases in DNA (G, A, C, and T) but can directly oxidize 8-oxoGua.[11] Another mode of •NO$_2$ reactivity involves the rapid bimolecular combination reactions with 8-oxoGua(−H)• or G(−H)• radicals described here. In DNA, the latter radicals are very long-lived even in the presence of oxygen. Our own laser flash photolysis studies have shown that, in oxygen-saturated solutions, the lifetimes of G(−H)• radicals in DNA are 0.2−0.6 s;[42] the lifetimes of 8-oxoGua(−H)• radicals in DNA are even longer and attain 3−15 s depending on the DNA secondary structure.[59] Thus, these radicals are targets for reaction with other reactive species, such as the •NO$_2$ radicals. In the case of the G(−H)• radicals, the nitro adducts that are formed can be considered as specific markers of •NO$_2$ radical reactions. In contrast, oxidation reactions dominate in the case of 8-oxoGua. The oxidative modifications of 8-oxoGua residues are highly mutagenic in vitro experiments.[60] The Gh lesions induce almost exclusive G → C transversions. The diastereoisomeric Sp lesions cause a mixture of G → T and G → C transversions, and the observed mutation frequencies were at least 1 order of magnitude higher than those caused by 8-oxoGua.[60]

Supporting Information Available: MS/MS spectra of spiro-iminodihydantoin nucleoside, analysis of the kinetics of 8-oxoGua oxidation by •NO$_2$ radicals, and NO$_2^-$ oxidation by G(−H)• radicals. This material is available free of charge via the Internet at http://pubs.acs.org.

JA044390R

(52) Ye, Y.; Muller, J. G.; Luo, W.; Mayne, C. L.; Shallop, A. J.; Jones, R. A.; Burrows, C. J. *J. Am. Chem. Soc.* **2003**, *125*, 13926−13927.
(53) Stanbury, D. M. In *Electron-Transfer Reactions*; Isied, S. S., Ed.; American Chemical Society: Washington, DC, 1997; Vol. 253, pp 165−182.
(54) Beckman, J. S.; Beckman, T. W.; Chen, J.; Marshall, P. A.; Freeman, B. A. *Proc Natl. Acad. Sci. U.S.A.* **1990**, *87*, 1620−1624.
(55) Lymar, S. V.; Hurst, J. K. *J. Am. Chem. Soc.* **1995**, *117*, 8867−8868.
(56) Lymar, S. V.; Hurst, J. K. *Inorg. Chem.* **1998**, *37*, 294−301.
(57) Ischiropoulos, H.; Beckman, J. S. *J. Clin. Invest.* **2003**, *111*, 163−169.
(58) Davis, K. L.; Martin, E.; Turko, I. V.; Murad, F. *Annu. Rev. Pharmacol. Toxicol.* **2001**, *41*, 203−236.
(59) Misiaszek, R.; Uvaydov, Y.; Crean, C.; Geacintov, N. E.; Shafirovich, V. *J. Biol. Chem.*, published online December 7, 2004 as manuscript M412253200.
(60) Henderson, P. T.; Delaney, J. C.; Muller, J. G.; Neeley, W. L.; Tannenbaum, S. R.; Burrows, C. J.; Essigmann, J. M. *Biochemistry* **2003**, *42*, 9257−9262.